

## Mechanical scratching induced phase transitions and reactions of boron carbide

著者	Chen Mingwei, McCauley James W.
journal or publication title	Journal of Applied Physics
volume	100
number	12
page range	123517
year	2006
URL	<a href="http://hdl.handle.net/10097/52472">http://hdl.handle.net/10097/52472</a>

doi: 10.1063/1.2405742

# Mechanical scratching induced phase transitions and reactions of boron carbide

Mingwei Chen<sup>a)</sup>

*International Frontier Center for Advanced Materials, Institute for Materials Research, Tohoku University, Sendai 980-8577, Japan*

James W. McCauley

*U.S. Army Research Laboratory, Aberdeen Proving Ground, Maryland 21005*

(Received 6 June 2006; accepted 26 October 2006; published online 27 December 2006)

The structural and chemical stabilities of single-crystal boron carbide ( $B_4C$ ) under severe mechanical scratching in air and water were investigated by transmission electron microscopy (TEM). Amorphous and nanocrystalline  $B_4C$  as well as nanostructured boron nitride (BN) were observed in the scratched fragments. Energy-filtered TEM analysis and thermodynamic calculations suggested that the BN nanophase results from the reaction of very small  $B_4C$  fragments with nitrogen in the ambience. © 2006 American Institute of Physics. [DOI: [10.1063/1.2405742](https://doi.org/10.1063/1.2405742)]

## I. INTRODUCTION

Over the last thirty years boron carbide (nominally  $B_4C$ ) ceramic has been developed for applications in body and light vehicle armors.<sup>1-3</sup> However, extensive shock experiments suggested that shock loading dramatically reduces the shear strength of  $B_4C$  at impact pressures above its Hugoniot elastic limit.<sup>4,5</sup> Various explanations for the shear strength loss have been proposed, including phase transitions, melting zones, and heterogeneous deformation.<sup>1,2,4-7</sup> Recently, high-resolution electron microscopy (HREM) of recovered  $B_4C$  fragments produced by ballistic testing revealed that the dramatic loss of shear strength results from the formation of 2–3 nm wide damage zones, in which the crystalline  $B_4C$  transforms into an amorphous phase.<sup>8</sup> Although these observations provide a compelling mechanism for the shear strength loss of  $B_4C$  under shock, the definitive description on the amorphization mechanism has not been achieved because three factors that may be favorable for the observed amorphization appear simultaneously during shock, i.e., multiaxial high pressures, fast loading/unloading, and high temperatures. Moreover, the difficulty in the recovery of shock-produced fragments with well-defined loading history restricts the systematic study of the amorphization mechanism.<sup>9</sup> As an alternative method, mechanical scratching by a sharp diamond tip has been demonstrated to produce high contact pressures, fast loading/unloading, and high temperatures,<sup>10-12</sup> which has some characteristics similar to shock loading. Although the loading process of scratching is difficult to quantify, the scratching tests can be simply performed under various environments. Moreover, the resultant fragments can be easily collected for postmortem characterization, which may provide valuable suggestions and clues for understanding the amorphization mechanism of  $B_4C$  under dynamic loading.

## II. EXPERIMENT

$B_4C$  single crystals grown by a floating zone technique were polished along (0001) faces by using 30 –0.1  $\mu\text{m}$  diamond films (South Bay Technology, Inc.). The finished surfaces for subsequent scratching experiments are mirrorlike and free of flaws. Energy-dispersive spectroscopy (EDS) and electron energy loss spectroscopy (EELS) measurements indicated that the single crystal contains boron, carbon, and traces of oxygen and silicon. The boron/carbon atomic ratio was determined to be  $\sim 3.9$ . Free carbon, boron nitride, and other secondary phases have not been found. Nanoindentation measurements indicated that the average hardness of the (0001)  $B_4C$  is  $\sim 43$  GPa, close to the literature values<sup>13,14</sup> and much lower than that of natural diamond.<sup>14</sup> A commercial scribe (Structure Probe, Inc.) was employed to scratch the prepolished  $B_4C$  surfaces in air and water, respectively. The scribe tip made from natural diamond is  $\sim 0.9$  mm in diameter with an exposed angle of  $90^\circ$ – $100^\circ$ . The radius of curvature at the tip is  $\sim 25$   $\mu\text{m}$ . In a dark room, sparks can be observed during scratching in air. The scratched debris particles were deposited onto holey  $\text{SiO}_2$  coated transmission electron microscopy (TEM) grids. Microstructural characterization was accomplished with a transmission electron microscope (Phillips CM-300, Phillips International, Inc.) equipped with a Gatan imaging filter (Gatan, Inc.).

## III. RESULTS AND DISCUSSION

The size of the scratched debris varies from tens of nanometers to several micrometers, and the debris particles generally aggregate together as shown in the bright-field TEM image [Fig. 1(a)], which was taken over a large area of the support grid. High-resolution electron microscopy revealed that the small fragments are composed of nanocrystalline particles embedded in an amorphous matrix [Fig. 1(b)]. The size of the nanocrystallites ranges from several to tens of nanometers. TEM EELS suggested that the boron/carbon ratios of both amorphous and nanocrystalline phases are  $\sim 3.8$ . Generally, the accuracy of TEM EELS measure-

<sup>a)</sup>Electronic mail: [mwchen@imr.tohoku.ac.jp](mailto:mwchen@imr.tohoku.ac.jp)

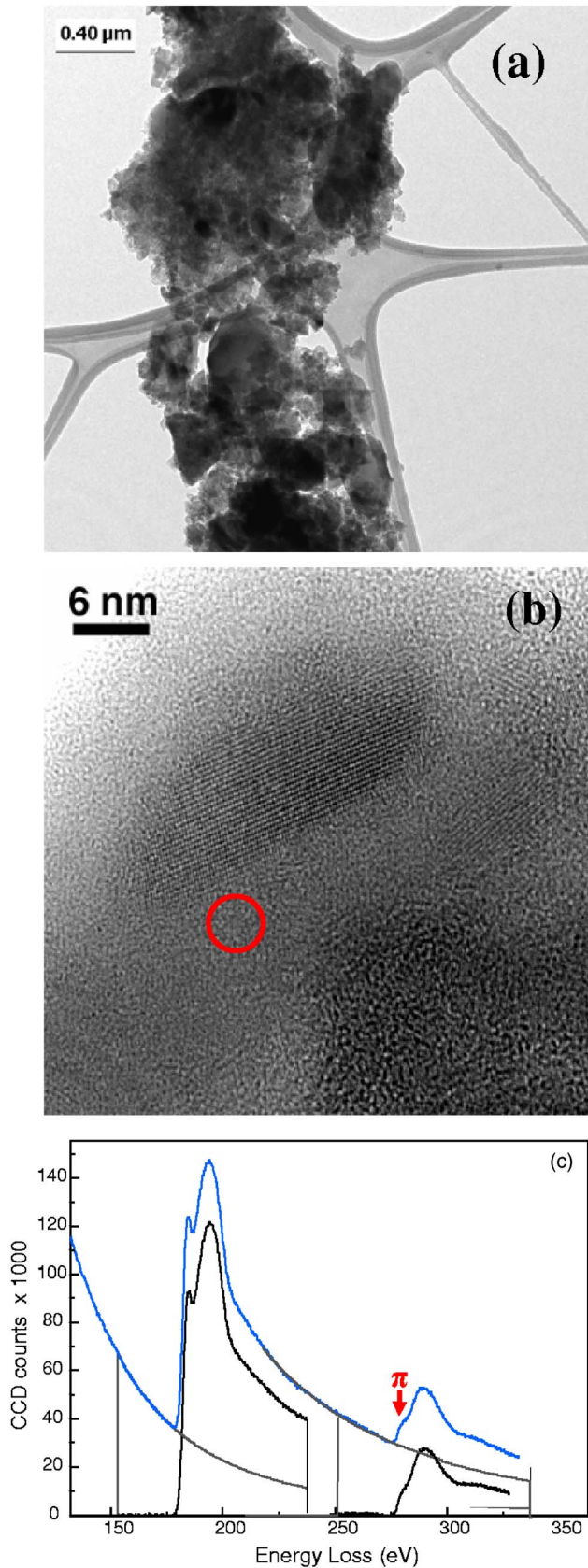


FIG. 1. (Color online) Microstructure and chemistry of  $B_4C$  fragments produced by scratching in air. (a) Bright-field TEM image of the scratched fragments, (b) HREM showing  $B_4C$  nanoparticles embedded in amorphous  $B_4C$  matrix, and (c) EELS spectrum of amorphous  $B_4C$  taken from the marked region in (b).

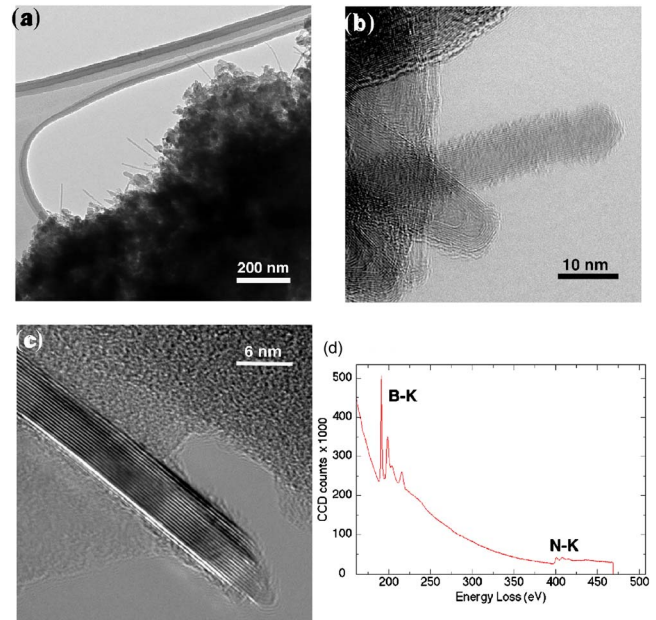


FIG. 2. (Color online) TEM characterization of scratched  $B_4C$  fragments and resulting BN nanotubes and nanowires. (a) A large scale observation of  $B_4C$  debris distributing on a holey  $SiO_2$  grid. A number of BN nanowires and nanotubes mixing with scratched debris can be observed. [(b) and (c)] HREM micrographs showing sharp and straight lattice fringes of a nanotube and a nanowire. (d) EELS spectrum taken from the portion of the tube [in Fig. 1(b)] suspended over a hole of  $SiO_2$  grid.

ments is of a few percents. Thus, the measured value is very close to that of the as-prepared single-crystalline  $B_4C$  [Fig. 1(c)], suggesting that the amorphous and nanocrystalline phases are formed through a polymorphic transition. Quantitative HREM measurements of the lattice spaces and angles of the nanocrystalline phase indicated that the nanocrystallites have a rhombohedral structure, which is the same as the precursor crystal  $B_4C$ . Intermediate phases with different crystal structures, as suggested by the high-pressure diamond anvil cell experiments,<sup>15</sup> have not been found. In addition, deformation defects, such as dislocations, deformation twins, and stacking faults cannot be found in the nanocrystalline  $B_4C$ . The EELS spectrum of the amorphous phase shows detectable carbon  $\pi$  edge [Fig. 1(c)], as reported before,<sup>11</sup> indicating the appearance of graphitelike  $sp^2$  carbon clusters that have been characterized in annealed amorphous  $B_4C$ .<sup>16</sup> The absence of the deformation defects and the formation of carbon clusters both indicate a possible temperature increase during mechanical scratching, which will be discussed later.

In addition to the fragments containing nanocrystalline and amorphous  $B_4C$ , nanotubes and nanowires mixing with the fine debris particles were occasionally found among the fragments produced by scratching in air [Fig. 2(a)]. These tubes and wires have a uniform diameter ranging from  $\sim 3$  to  $\sim 10$  nm and a length of up to hundreds of nanometers. The debris particles around the nanotubes and nanowires were identified to be amorphous carbon and nanocrystalline  $B_4C$ . HREM observations, for example, Figs. 2(b) and 2(c), suggested that the nanowires and nanotubes exhibit a layer structure with sharp lattice fringes. The lattice-fringe space was determined to be about  $3.3 \text{ \AA}$ , which is consistent with the (0001) interplanar distance of  $3.33 \text{ \AA}$  in hexagonal

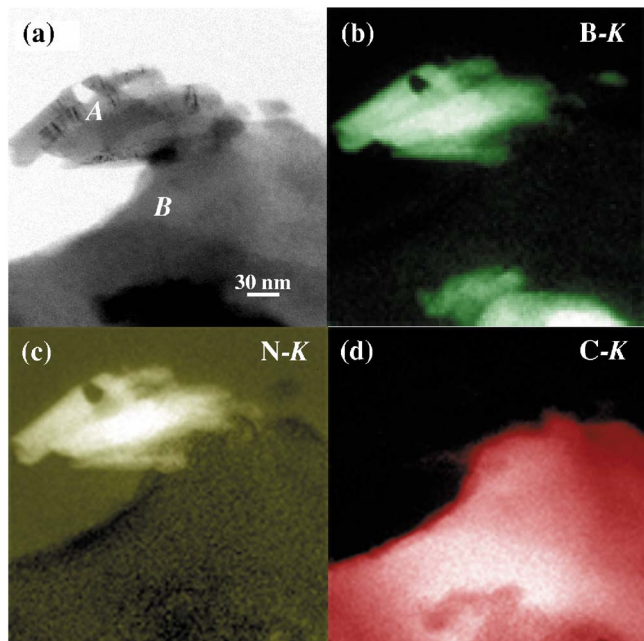
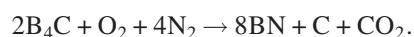


FIG. 3. (Color online) Coexistence of BN nanowires (A), amorphous carbon (B), and  $B_4C$  remainder within one region. (a) Energy-filtered bright-field TEM image showing a portion of a tiny fragment. [(b)–(d)] Elemental maps of boron, nitrogen, and carbon taken from their  $K$  edges, suggesting the enrichment of boron and nitrogen in region A, carbon in region B, and carbon and boron in region C.

boron nitride (BN).<sup>17</sup> The chemical composition of individual nanotubes and nanowires was determined by TEM EELS. The spectra, for example, Fig. 2(d), were taken from the portions of nanotubes and nanowires suspended over a hole in a holey  $SiO_2$  grid. Only two distinct absorption edges are present, corresponding to the known  $K$  edges of boron at 188 eV and nitrogen at 401 eV. The near edge fine structures of the  $K$  edges in the spectrum are consistent with the hexagonal  $sp^2$  bonding between boron and nitrogen. Quantitative chemical analysis of the nanowire/nanotube EELS spectra indicated that the B/N atomic ratio is  $\sim 1.1$ , which is very close to the stoichiometry of BN.

In order to understand the formation mechanism of the nanostructured BN, an EELS approach including the collection of multiple energy-filtered images [Figs. 3(a)–3(d)] was used to display the distributions of carbon, nitrogen, and boron. The intensity contrast, bright and dark, reflects the relative element concentrations. The chemical maps shown in Figs. 3(b)–3(d) suggest the coexistence of three phases with different chemical compositions, i.e., a boron/nitrogen-rich phase, a carbon-rich phase, and a carbon/boron-rich phase, within one region. Using HREM and EELS, these phases were further determined to be BN nanowire ropes in region A, amorphous carbon in region B, and the  $B_4C$  remainder in region C [Figs. 4(a)–4(d)]. The appearance of the BN nanowires and amorphous carbon suggests a possible chemical reaction between  $B_4C$  and air (21%  $O_2$  and 78%  $N_2$ ) during scratching, i.e.,



The change of the Gibbs free energy of this reaction was calculated to be negative at temperatures below 3600 K and

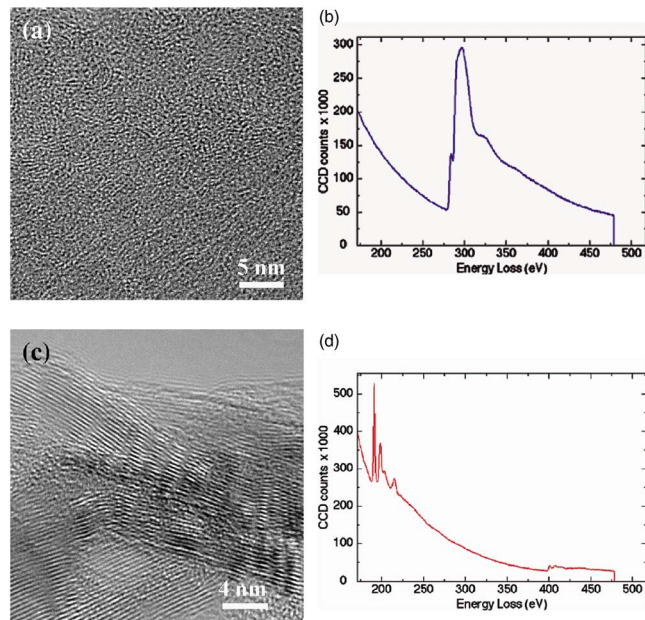


FIG. 4. (Color online) (a) HREM image of region B in Fig. 3(a), showing amorphous feature, (b) EELS spectrum of region B, suggesting that this region only contain carbon, and [(c) and (d)] HREM image and EELS spectrum taken from region A. The phase containing boron and nitrogen is characterized to be a bunch of BN nanowires.

$\sim -421$  kJ/mol at 2734 K (the melting point of  $B_4C$ ), suggesting that this reaction is thermodynamically preferred over a wide temperature range. It is well known that the collision of two hard materials during scratching can generate intense heat associated with concentrated plastic and fracture work. The release of these mechanical energies applied to tiny debris over a very short time scale can produce high temperatures that facilitate the reaction of  $B_4C$  with air. Carbon and boron both have a strong affinity for oxygen and their oxides have large formation heats. The absence of boron oxides revealed by extensive TEM inspection indicates that the reaction between carbon and oxygen occurs prior to the formation of BN, which consumes oxygen and carbon and creates a nitrogen and boron coenriched atmosphere. The fact that BN nanotubes can be synthesized from elemental boron in a nitrogen atmosphere at high temperatures strongly suggests that the formation of nanostructured BN is promoted by the nitrogen and boron enriched ambience.<sup>18</sup> The creation of nanotubes and nanowires as opposed to coarse BN crystals may result from the fact that the mechanical scratching only provides a harsh environment with limited boron sources, which prevents substantial crystal growth and only produces nanosized crystals. The appearance of both nanotubes and nanowires may be due to the heterogeneous environments produced by the mechanical scratching.

To test the proposed reaction, the mechanical scratching of  $B_4C$  was performed in distilled water. In this case, BN and amorphous carbon were not detected, indirectly supporting the proposed reaction. Among the fragments, very small debris particles were observed to contain nanocrystalline  $B_4C$  particles surrounded by a 2–4 nm thick amorphous layer [Figs. 5(a) and 5(b)]. Apparently, the water surroundings not only effectively prevent the decomposition of  $B_4C$  debris but

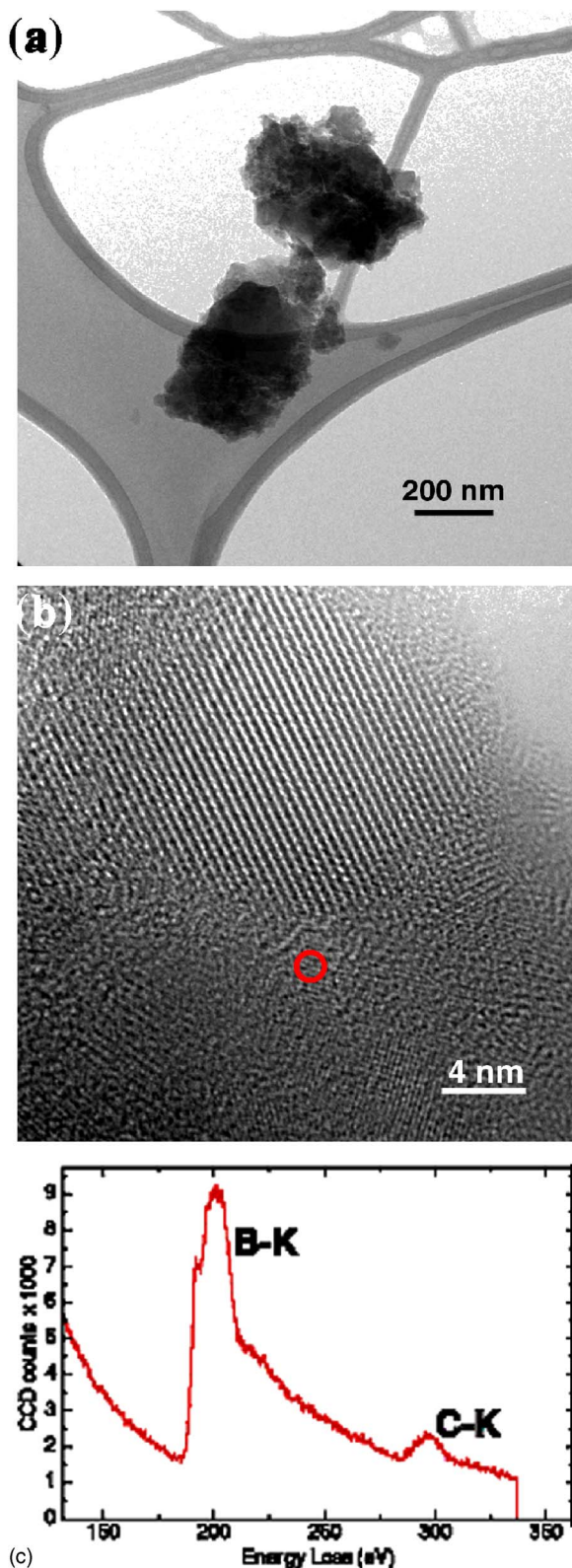


FIG. 5. (Color online) Microstructure and chemistry of  $B_4C$  fragments produced by scratching in distilled water. (a) Bright-field TEM micrograph of fine debris particles. (b) HREM observation showing nanocrystalline  $B_4C$  with a 2–4 nm amorphous outer layer. (c) EELS spectrum taken from the amorphous phase showing both carbon and boron  $K$  edges.

also suppress the amorphization of  $B_4C$  because the amount of amorphous phase is much less than that observed in air-scratched fragments. TEM EELS characterization shows that the boron/carbon ratio of the thin amorphous layers is  $\sim 3.9$

[Fig. 5(c)], close to that of crystalline  $B_4C$ . Unlike that of the air-scratched amorphous  $B_4C$ , the near edge fine structure of carbon  $K$  edge of the amorphous  $B_4C$  produced by scratching in water does not definitively show a  $\pi$  band [Fig. 5(c)]. Thus, the appearance of the carbon  $\pi$  band in the air-scratched amorphous  $B_4C$  most likely results from the significant temperature increase, as demonstrated by recent high-temperature Raman study.<sup>16</sup> Surprisingly, deformation defects, such as dislocations, deformation twins, and stacking faults, are rarely seen in the water-scratched  $B_4C$  fragments, similar to those in the air-scratched fragments. Although the localized temperature increase during the formation of very small fragments may not be completely suppressed by water cooling, the temperature increase should be very limited because the known formation temperature of  $sp^2$  carbon clusters in amorphous  $B_4C$  is in the range between  $300^\circ$  and  $600^\circ C$ , which is far below the recovery/recrystallization temperature of  $B_4C$  ( $\sim 1200^\circ C$ , half of the melting point<sup>19</sup>). Thus, the absence of the deformation defects may not be due to the annealing (or temperature) effect, and the scratch-induced amorphization of  $B_4C$  is more likely driven by high stresses, rather than plastic deformation.

#### IV. SUMMARY

In summary, scratch-induced amorphization, nanocrystallization, and chemical reactions of  $B_4C$  in water and air were investigated by HREM and EELS. It was revealed that the amorphization of  $B_4C$  appears to be associated with both high stresses and high temperatures. Furthermore, BN nanowires and nanotubes were found in air-scratched  $B_4C$  fragments, which may offer a mechanical approach for synthesizing nanostructured BN in addition to the known physical and chemical methods.

#### ACKNOWLEDGMENTS

This work was supported by a Grant-in-Aid-A for Scientific Research from Japan Society of the Promotion of Science (JSPS) through Tohoku University and by U.S. Army Research Laboratory through Johns Hopkins University.

<sup>1</sup>D. E. Grady, Report No. SAND 94–3266 (Sandia National Laboratory, Albuquerque, 1995).

<sup>2</sup>D. P. Dandekar, Report No. ARL-TR-2456 (Army Research Laboratory, Aberdeen, 2001).

<sup>3</sup>M. W. Chen, J. W. McCauley, J. C. LaSalvia, and K. J. Hemker, *J. Am. Ceram. Soc.* **88**, 1935 (2005).

<sup>4</sup>D. E. Grady, *J. Phys. IV* **4**, C8 (1994).

<sup>5</sup>N. K. Bourne, *Proc. R. Soc. London, Ser. A* **458**, 1999 (2002).

<sup>6</sup>T. Mashimo and M. Uchino, *J. Appl. Phys.* **81**, 7064 (1997).

<sup>7</sup>T. J. Vogler, W. D. Reinhart, and L. C. Chhabildas, *J. Appl. Phys.* **95**, 4173 (2004).

<sup>8</sup>M. W. Chen, J. W. McCauley, and K. J. Hemker, *Science* **299**, 1563 (2003).

<sup>9</sup>M. W. Chen, J. W. McCauley, D. P. Dandekar, and N. K. Bourne, *Nat. Mater.* **5**, 614 (2006).

<sup>10</sup>K. Minowa and K. Sumino, *Phys. Rev. Lett.* **69**, 320 (1992).

<sup>11</sup>D. Ge, V. Domnich, T. Juliano, E. A. Stach, and Y. Gogotsi, *Acta Mater.* **52**, 3921 (2004).

<sup>12</sup>F. M. van Bouwelen, J. E. Field, and L. M. Brown, *Philos. Mag.* **83**, 839 (2003).

<sup>13</sup>V. Domnich, Y. Gogotsi, M. Trenary, and T. Tanaka, *Appl. Phys. Lett.* **81**, 3783 (2002).

- <sup>14</sup>P. F. Mcmillan, Nat. Mater. **1**, 19 (2002).
- <sup>15</sup>M. Manghnani, PAC RIM 4 Conference, Maui, Hawaii, 2001 (unpublished), Paper No. PAC6-B-10-2001.
- <sup>16</sup>X. Q. Yan, W. J. Li, T. Goto, and M. W. Chen, Appl. Phys. Lett. **88**, 131905 (2006).
- <sup>17</sup>N. G. Chopra, R. J. Luyken, K. Cherrey, V. H. Crespi, M. L. Cohen, S. G. Louie, and A. Zettl, Science **269**, 966 (1995).
- <sup>18</sup>R. S. Lee, J. Gavillet, M. Lamy de la Chapelle, A. Loiseau, J.-L. Cochon, D. Pigache, J. Thibault, and F. Willaime, Phys. Rev. B **64**, 121405 (2001).
- <sup>19</sup>F. J. Humphreys and M. Hatherly, *Recrystallization and Related Annealing Phenomena* (Pergamon, New York, 1995).